Progress In Electromagnetics Research, PIER 91, 153–171, 2009

A FAST APPROACH FOR SIMULATING LONG-TIME RESPONSE OF HIGH-SPEED DISPERSIVE AND LOSSY INTERCONNECTS TERMINATED WITH NONLINEAR LOADS

C.-N. Chiu

Department of Electrical Engineering
Da-Yeh University
112, Shanjiao Rd., Dacun, Changhua, Taiwan 51591, ROC

I.-T. Chiang

Lorentz Solution, Inc.
1900, McCarthy Blvd., Suite 208, Milpitas, CA 94539, USA

Abstract—This paper presents an efficient approach for analyzing the long-time response of high-speed dispersive and lossy interconnects terminated with nonlinear loads. In this approach, a fast real-time convolution algorithm with computational cost $O(N \log^2 N)$ is suggested to tackle the long-time analysis of the high-speed dispersive and lossy interconnects, which are modeled by S-parameters. In addition, the acquirement of the S-parameters is recommended to adopt wideband closed-form formulas. The time response of a microstrip line with a nonlinear load is shown as a practical example. The dominant parameters affecting the response of this microstrip line is observed and discussed in detail. The approach demonstrates its efficiency and accuracy in the analysis.

1. INTRODUCTION

The trend toward increasing the speed of modern digital systems makes the requirement for signal integrity (SI) more stringent than ever before. Signal integrity is also more troublesome to achieve in the face of this requirement. Typically, the higher is the speed of a digital signal, the wider is its frequency spectrum. As a consequence, the dispersive and lossy effects of the digital signal propagating

Corresponding author: C.-N. Chiu (cnchiu@mail.dyu.edu.tw).

along an interconnect can be very pronounced and can worsen its SI performance. Among SI failures, perhaps the intersymbol interference (ISI) [1, 2] irritates most as the signal speed gets higher and the period becomes shorter. ISI, interference among the symbols of the signal, is caused predominantly by signal reflections at the loads of an interconnect. To capture the full effects of ISI, it is important to thoroughly analyze a long-time response persisting for tens of symbols. In addition to high-speed digital devices, the high-frequency/high-speed mixed analog-digital devices are being widely applied in modern electronic systems. Thus, the dispersive and lossy interconnects are more and more often terminated with nonlinear loads. However, few numerical approaches can efficiently analyze such a long-time response. The accurate analysis could be very time-consumptive and not be acceptable when a large amount of such interconnects are involved in practice.

Accurate analysis of dispersive and lossy interconnects terminated with nonlinear loads has been a dilemma for decades. Analysis of a dispersive and lossy interconnect is straightforward in the frequency domain, but examination of its nonlinear loads is convenient in the time domain. The finite-difference time-domain (FDTD) method [3–7] has been proposed to solve this issue directly in the time domain. However, it is not efficient for long-time analysis of high-speed interconnects owing to the Courant condition. In addition, the late-time instability of the FDTD method may occur, especially when both the dispersive and lossy properties are considered at the same time. In general, the FDTD method is not a reliable and simplified means for this purpose.

On the other hand, time-frequency transform methods [8–17] have become popular for this purpose. These methods are more straightforward and make it easier to model the arbitrarily dispersive and lossy properties of an interconnect. The nonlinear loads, however, prevent carrying out the convolution by the fast Fourier transform (FFT) from these methods because FFT cannot be applied directly in this situation. As a result, for N sampling points, the direct convolution at $O(N^2)$ instead of $O(N \log N)$ utilizing FFT is mandatory in order to implement the convolution between the nonlinear terminations and the linear part.

In this paper, the long-time response of high-speed dispersive and lossy interconnects terminated with nonlinear loads is analyzed. An efficient approach is proposed to resolve this problem based on the wideband closed-form formulas for expressing the S-parameters of interconnects and the fast real-time convolution (FRTC) algorithm [18, 19], which originates from the idea in [20]. The computation time of the S-parameters by the formulas is in a

flash. In addition, the FRTC can perform the convolution for the interconnects terminated with nonlinear loads at the computational cost $O(N \log^2 N)$, which is a significant improvement over the conventional $O(N^2)$ algorithm. Thus, the approach is rather efficient when analyzing the long-time response of high-speed dispersive and lossy interconnects terminated with nonlinear loads.

Using this efficient approach, the numerical results of the time response of a dispersive and lossy microstrip line with a nonlinear load are obtained and shown as an example. The structure of the microstrip line is very common and is widely applied as interconnects in printed circuit boards (PCBs), packages, and chips. Today's high-speed digital signals propagating along this kind of interconnect may suffer more lossy effects owing to conductor and dielectric losses, as well as more dispersive effects caused by current redistribution and wave-mode coupling [21]. These effects can seriously aggravate SI performance, and may make the analysis valueless if such effects are not taken into account.

To save considerable time in performing a simulation, accurate wideband closed-form formulas for describing the S-parameters of a microstrip line were suggested in the analysis. The improved formulas are listed in the appendix and have been well validated by a full-wave numerical method. Analysis of the time response is not trivial and therefore requires a thorough simulation. As expected in the simulation, the distortion of signals in a dispersive and lossy microstrip line terminated with a nonlinear load is clear and appreciable. The signal distortion may depend on line properties, load characteristics, and source features. On the basis of the analysis, the dominant parameters for influencing the distortion can be clearly predicted.

2. FORMULATION

Figure 1 shows a high-speed dispersive and lossy interconnect with a nonlinear load. This configuration is composed of a linear two-port interconnect, a voltage source $v_g(t)$ with internal impedance Z_g, and a nonlinear load. For the linear two-port interconnect, the S-parameters may be found by using numerical methods, measurement, or closed-form formulas. For the analysis here, the S-parameters are commendable for describing the two-port interconnect in contrast with other parameters [10]. A set of improved wideband and accurate closed-formulas for microstrip lines is listed in the appendix. It is the most efficient way to obtain the S-parameters.

If the nonlinear load can be described by

$$i_2(t) = -f(v_2(t)), \tag{1}$$

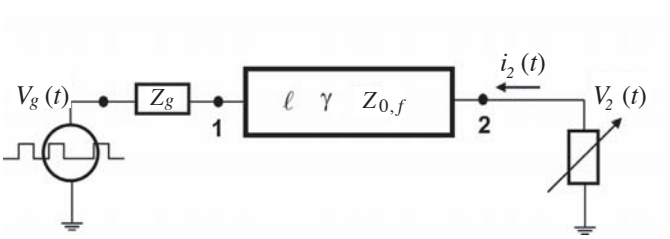

Figure 1. Configuration of a high-speed dispersive and lossy interconnect with a nonlinear load.

the time-domain nonlinear equation at Port 2 may be derived to

$$f(v_2(t)) = x(t) * v_2(t) + y(t). \tag{2}$$

In (2),

$$x(t) = F^{-1}\left\{\frac{4Z_gS_{12}S_{21} - Z_g\Delta_1\Delta_2 - Z_r\Delta\Delta_2}{Z_r\Delta(Z_r\Delta + Z_g\Delta_1)}\right\}, \tag{3}$$

$$y(t) = F^{-1}\left\{\frac{2V_gS_{21}}{Z_r\Delta + Z_g\Delta_1}\right\} \tag{4}$$

where

$$\Delta = (1+S_{11})(1+S_{22}) - S_{12}S_{21}, \tag{5}$$

$$\Delta_1 = (1-S_{11})(1+S_{22}) + S_{12}S_{21}, \tag{6}$$

$$\Delta_2 = (1+S_{11})(1-S_{22}) + S_{12}S_{21}. \tag{7}$$

In (3) and (4), V_g denotes the Fourier transform of the voltage source $v_g(t)$; F^{-1} denotes the inverse Fourier transform and "$*$" stands for convolution. S_{11}, S_{12}, S_{21}, and S_{22} are the S-parameters of the interconnect. Z_g and Z_r are the source impedance and the reference impedance at ports, respectively. By direct convolution, the computational cost of (2) is $O(N^2)$, which is exorbitant when the time response is long or when the response is oversampled to avoid the notorious aliasing. To expedite the convolution, we apply the FRTC algorithm as described in the following paragraphs.

To perform the real-time convolution, we must use the entire history of the convoluted signal. The key to speeding up this process is to take advantage of the previously-solved unknowns of $v_2(t)$. Since these unknowns have already been solved, the convolution for this part can be performed by FFT back and forth instead of by the direct convolution. By applying this idea recursively, the cost for the real-time convolution is reduced to the computational cost $O(N\log^2 N)$, which is a big improvement over the $O(N^2)$ cost.

The procedure and cost of the FRTC algorithm are illustrated in Fig. 2 as a flow chart for solving (2). Here, the convolution in (2) can be written as

$$x(t) * v_2(t) = \sum_{j=0}^{i} x^{i-j} v_2^j, \quad t = i\Delta t, \quad t' = j\Delta t \tag{8}$$

where Δt is the time step. First, we solve a few unknowns (power of 2 to be exact) of (2) by the direct convolution in Step I. Next, we recycle the solved unknowns in Step I and perform the convolution by FFT back and forth in Step II. As mentioned earlier, the convolution relies on both the present time and the previous history. Thus, Step II accounts for the contribution from the history for later time steps, and this part can be accelerated by FFT. Then, the convolution continues as Step III by utilizing the results of Step II. Steps IV, V, VI and VII are performed likewise. The divide-and-conquer procedure continues as the blank "squares" and "triangles" in Fig. 2. In the "squares", we take the advantage of FFT, which is the key to accelerating the convolution. Note that it will be one big triangle in Fig. 2 for the direct convolution not applying the FRTC algorithm. It means that the direct convolution does not take advantage of any solved unknowns of $v_2(t)$ and it results in an inefficient $O(N^2)$ algorithm.

The cost of the direct convolution is shown as a "triangle" in Fig. 2 (Steps I, III, V and VII). The cost of the convolution by FFT back and forth is shown as a "square" in Fig. 2 (Steps II, IV, and VI). The cost of a "triangle" is $O(m)$, $m = p\,(p+1)/2$ and p is the number of points

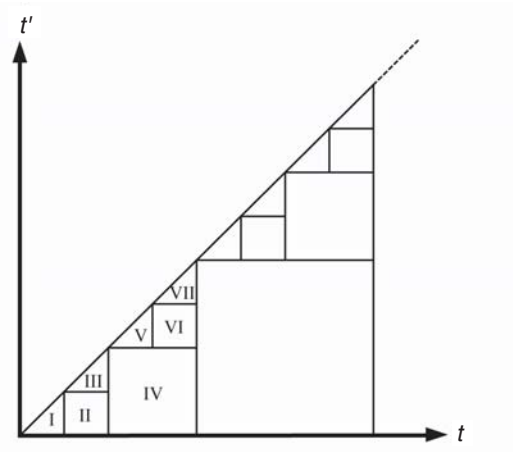

Figure 2. Flow chart of the FRTC algorithm in first few steps.

for the direct convolution. The cost of a "square" is $O(n \log n)$ and n varies depending on the different time steps. Apparently, the larger the "square" is (or the longer the response is), the more time is saved by the FRTC. When there are $2N$ points in total and N is large, the cost is

$$O\left(N \log N + 2\left(\frac{N}{2} \log \frac{N}{2}\right) + 4\left(\frac{N}{4} \log \frac{N}{4}\right) + \ldots\right) = O(N \log^2 N). \quad (9)$$

To achieve the best performance, the number of time steps for the direct convolution must be carefully determined. It is deduced that 32 or 64 is the optimal choice [18]. It is worth mentioning that the mismatch between $Z_{0,f}$ and Z_r of the interconnect described by S-parameters may greatly increase the response time [15]. Under this circumstance, if this mismatch cannot be avoided, the FRTC can save even more computational cost than the direct convolution.

3. RESULTS AND DISCUSSION

The long-time response of a high-speed dispersive and lossy microstrip line with a nonlinear load is studied using the approach mentioned earlier. The geometry of a typical microstrip line is shown in Fig. 3. W, H, and T denote the strip width, substrate thickness, and strip thickness, respectively. In addition, ε_r, $\tan\delta$, σ_c, and μ_c indicate the dielectric constant of the substrate, the loss tangent of the substrate, the conductivity of the conductor, and the permeability of the conductor, respectively. For this line, the S-parameters can be obtained by using closed-form formulas. Applying such formulas can save much time in performing simulations and also can clearly distinguish the physical mechanisms between dispersion and losses. An improved set of accurate wideband closed-form formulas is listed

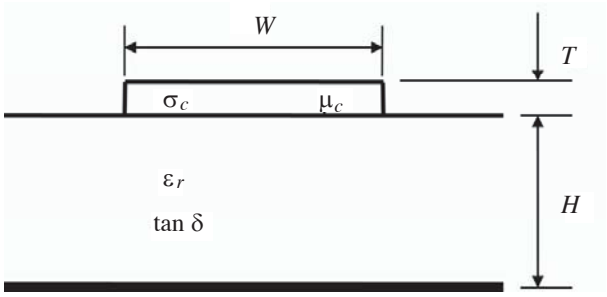

Figure 3. Dimensions and parameters of a microstrip line.

in the appendix. These closed-form formulas, found in the literature, have been modified here to obtain better accuracy for a wider frequency band, which has been validated. As shown in Fig. 4, the S-parameters of a dispersive and lossy microstrip line by using these formulas are in good agreement with those computed by IE3D, a method of moments (MoM) full-wave field solver. The microstrip line with its specified dimensions and parameters in Fig. 4 is the basis for the following analysis and discussion.

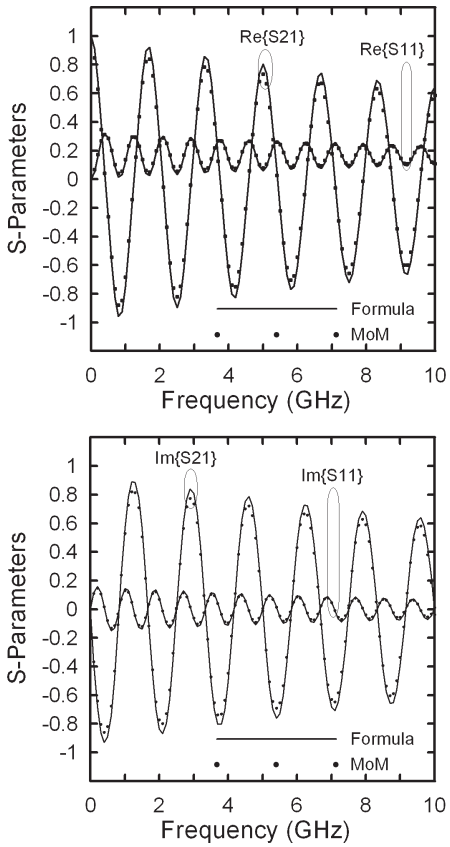

Figure 4. Accuracy test for the closed-form formulas. $W = 0.2\,\text{mm}$, $H = 0.2\,\text{mm}$, $T = 0.01\,\text{mm}$, $\ell = 0.1\,\text{m}$, $\varepsilon_r = 4.5$, $\tan\delta = 0.025$, $\sigma_c = 5.8 \times 10^7\,\text{S/m}$, $\mu_c = 4\pi \times 10^{-7}\,\text{H/m}$, and $R_r = 50\,\Omega$.

Two loads at Port 2 are considered. The first load is a resistance R_L in series with a nonlinear device. The nonlinear equation of this

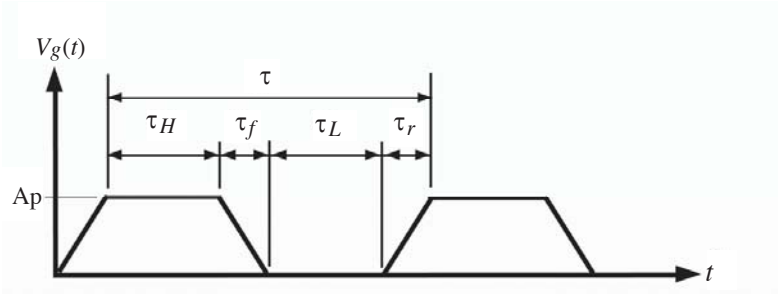

Figure 5. Trapezoidal-pulse train.

device is written as

$$i(t) = I_S \left[\exp\left(\frac{v(t)}{V_T} \right) - 1 \right] \tag{10}$$

where $i(t)$ is the current (in amperes) passing through the device, $v(t)$ is the voltage (in volts) at the device, and $V_T = 0.025$ volts. In this paper, the saturation current, I_S, is assumed to be 10^{-15}A except in Fig. 10, and the resistance, R_L, is assumed to be $10\,\Omega$ except in Fig. 9. The second load is the static impedance, $Z_{0,0}$, of the microstrip line. This load is quasi-matched to the considered line but cannot be exactly matched because of the dispersive and lossy nature of the line.

The voltage source at Port 1 generates a trapezoidal-pulse train. The associated parameters of each trapezoidal pulse are defined in Fig. 5. In the following analysis and discussion, the pulse number of the train is assumed to be 5. In addition, the pulse train is launched at $t = 0$ and its duty cycle is 50%. For all the following analyses, the internal impedance Z_g of the source is assumed to be $30\,\Omega$ and the time response is observed at Port 2. Numerical results for showing this response are computed by the FRTC algorithm. The computation time by this algorithm is much shorter than that by the direction convolution algorithm. The computation time means the duration of all the S-parameter computations, all the S-parameter transformations from the frequency domain into the time domain, the nonlinear iterations and the realtime convolution. For the computation of the nonlinear-load case in Fig. 6(a) having 131072 sampling points, the computation time by the direct convolution algorithm is 4243 seconds when using a 1.73-GHz Pentium IV processor to compute a 1000-ns response. In contrast to such a long time, the computation time by the FRTC algorithm is only 110 seconds, which is a thirty-nine times improvement. In addition, it is worth of mentioning that

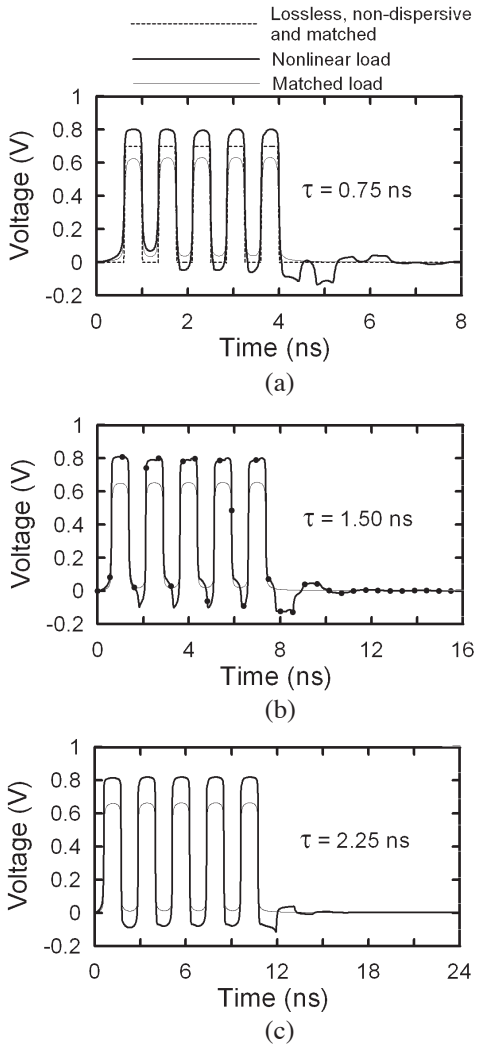

Figure 6. Analysis with period τ as a parameter. $A_p = 1\,\mathrm{V}$, $\tau_r = \tau_f = 35\,\mathrm{ps}$. (a) $\tau = 0.75\,\mathrm{ns}$, $\tau_H = \tau_L = 0.34\,\mathrm{ns}$; (b) $\tau = 1.5\,\mathrm{ns}$, $\tau_H = \tau_L = 0.715\,\mathrm{ns}$; (c) $\tau = 2.25\,\mathrm{ns}$, $\tau_H = \tau_L = 1.09\,\mathrm{ns}$.

the computation time for the S-parameters obtained by the closed-formed formulas is less than one second.

Figure 6 shows the time response with the period τ of the pulse train as a parameter. An accuracy test is given for a matched lossless and non-dispersive microstrip line having dimensions and a dielectric

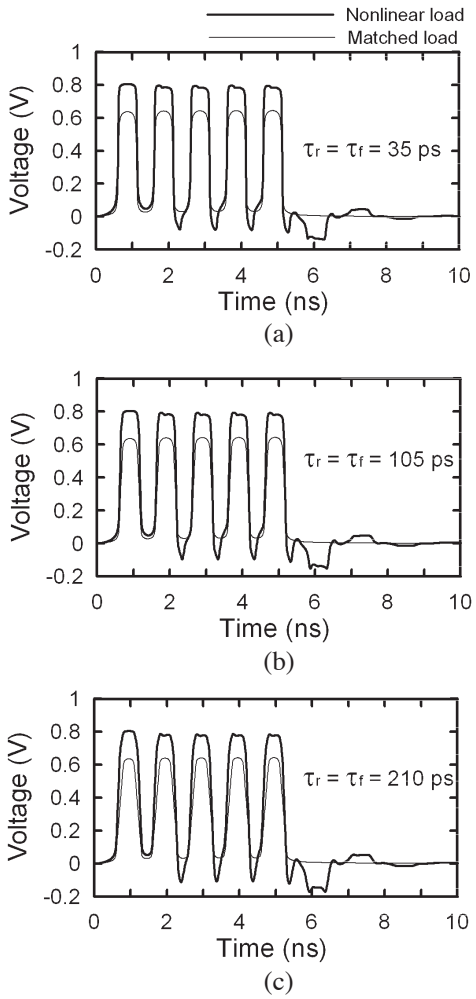

Figure 7. Analysis with equal rise time τ_r and fall time τ_f as a parameter. $A_p = 1\,\text{V}$, $\tau = 1\,\text{ns}$. (a) $\tau_H = \tau_L = 0.465\,\text{ns}$, $\tau_r = \tau_f = 35\,\text{ps}$; (b) $\tau_H = \tau_L = 0.395\,\text{ns}$, $\tau_r = \tau_f = 105\,\text{ps}$; (c) $\tau_H = \tau_L = 0.29\,\text{ns}$, $\tau_r = \tau_f = 210\,\text{ps}$.

constant the same as the line in Fig. 4. This computed result, shown as the dashed line in Fig. 6(a), is exactly equal to the analytical solution of this line. Another accuracy test is given for a dispersive and lossy microstrip line terminated with a nonlinear load in Fig. 6(b). The computed results are in good agreement with the results computed by the traditional direct convolution, shown as discrete dots. In Fig. 6 and

all the following figures, the thin solid line denotes the quasi-matched load case while the thick solid line indicates the nonlinear load case. It is obvious that the undesired distortion is much more serious in the nonlinear load case. However, both the high- and low-level hold times are shortened even in the quasi-matched load case. Physically, the frequencies in the spectrum of the pulse train propagate at different velocities and the higher frequencies suffer more loss in the dispersive and lossy microstrip line. As a result, every pulse is rounded and broadened. The distortion caused by ISI can be appreciable when the microstrip line is terminated with a nonlinear load, especially as the period is not large enough. For example, the voltage levels may overshoot or undershoot. In addition, the rise and fall times may be jittered manifestly. A practical rule suggests that the influence of ISI is reduced when the period is larger than two times the propagation delay of the line. However, following such a rule may be very risky. As shown in Fig. 6(c), where the period is much larger than two times the propagation delay (about 0.6 ns), the ISI is still large. Consequently, the analysis of modern high-speed interconnects should not be based on a rule, but requires a complete simulation instead.

The influence of the variation in rise and fall times is shown in Fig. 7. The period of the pulse train is fixed here. It is obvious that this influence is much less than that caused by the variation in period, even though speeding up the rise and fall times may worsen the impedance matching of the line. Fig. 8 shows the time response with the pulse amplitude A_p as a parameter. The magnitude of the observed pulses in the quasi-matched load case varies linearly with respect to the variation in the amplitude. However, the pulses in the nonlinear load case may be highly distorted owing to the huge variation in the nonlinear characteristic of the load. As this figure shows, the SI performance could be destroyed when assigning improper pulse amplitudes.

The series resistance R_L of the nonlinear load may provide a tuning parameter for reducing the distortion, as shown in Fig. 9. This resistance may result from chip contacts, bonding wires, package pins, PCB interconnects, and/or resistors. If this resistance is neglected during simulation, the SI performance could be totally different in a real situation. In addition, the SI performance can be improved, from a positive viewpoint, by properly controlling this resistance.

Using similar nonlinear devices having different saturation currents may cause totally different distortion. Fig. 10(a) shows that the distortion in the nonlinear-load case mainly results in the overshooting defect, while Fig. 10(c) shows that the distortion primarily causes the undershooting defect. In contrast to these two

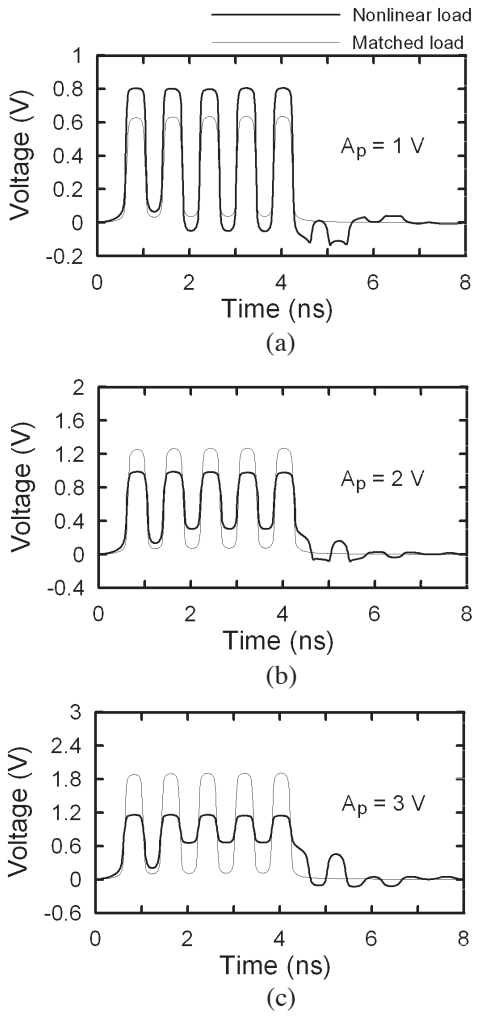

Figure 8. Analysis with amplitude A_p as a parameter. $\tau = 0.8\,\text{ns}$, $\tau_r = \tau_f = 70\,\text{ps}$, $\tau_H = \tau_L = 0.33\,\text{ns}$. (a) $A_p = 1\,\text{V}$; (b) $A_p = 2\,\text{V}$; (c) $A_p = 3\,\text{V}$.

cases, Fig. 10(b) shows that the SI performance could be good. Again, these results demonstrate that the SI performance in the nonlinear load case cannot be predicted by a simple means.

To summarize these analyses, the period and amplitude of a pulse train are the dominant parameters influencing the SI performance when the microstrip line is terminated with a nonlinear load. From a

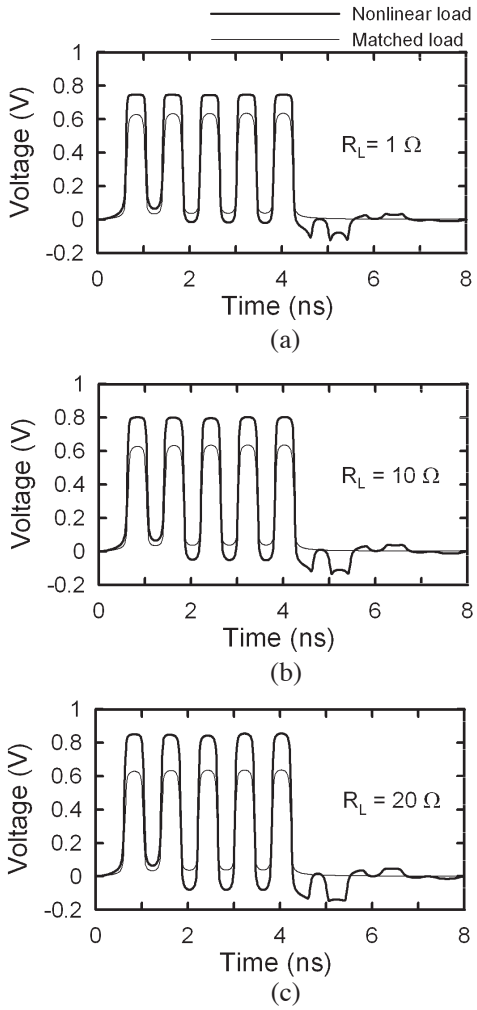

Figure 9. Analysis with resistance R_L in the nonlinear load as a parameter. $A_p = 1\,\mathrm{V}$, $\tau = 0.8\,\mathrm{ns}$, $\tau_r = \tau_f = 70\,\mathrm{ps}$, $\tau_H = \tau_L = 0.33\,\mathrm{ns}$. (a) $R_L = 1\,\Omega$; (b) $R_L = 10\,\Omega$; (c) $R_L = 20\,\Omega$.

practical design aspect, the distortion caused by improperly choosing these parameters should be carefully analyzed and avoided, based on an overall simulation. In addition, the series resistance of the nonlinear load is a convenient tuning parameter. Proper tuning of this resistance may be an easy and flexible way to reduce the distortion, especially after the final fabrication.

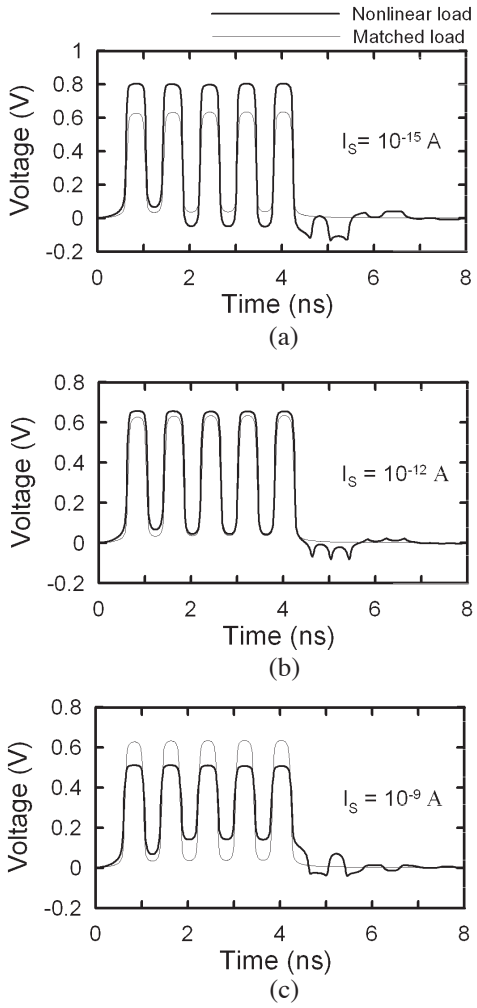

Figure 10. Analysis with saturation current I_S of the nonlinear load as a parameter. $A_p = 1\,\mathrm{V}$, $\tau = 0.8\,\mathrm{ns}$, $\tau_r = \tau_f = 70\,\mathrm{ps}$, $\tau_H = \tau_L = 0.33\,\mathrm{ns}$. (a) $I_S = 10^{-15}\,\mathrm{A}$; (b) $I_S = 10^{-12}\,\mathrm{A}$; (c) $I_S = 10^{-9}\,\mathrm{A}$.

4. CONCLUSION

An efficient approach, accelerated by the closed-form formulas and the FRTC algorithm, has been proposed to compute the long-time response of high-speed dispersive and lossy interconnects terminated

with nonlinear loads. The implemented computer code is much more efficient than traditional methods. Based on this approach, the SI performance of a dispersive and lossy microstrip line terminated with a nonlinear load is studied and discussed in detail. This response is complicated and should not be underestimated even for a single microstrip line. Because this response depends not only on the source and load features but also on the nature of the line, a thorough simulation should be performed to analyze such a phenomenon. The proposed approach can be further extended to tackle any kinds of multiconductor interconnects terminated with arbitrary nonlinear loads.

APPENDIX A.

A set of accurate wideband closed-form formulas for expressing the S-parameters of a microstrip line has been carefully selected from the literature and is listed here. In addition, we have slightly modified these formulas to achieve better accuracy and to make them more suitable for the SI analysis. The geometry of the microstrip line is shown in Fig. 3. W, H, and T denote its strip width (in millimeters), its substrate thickness (in millimeters), and its strip thickness (in millimeters), respectively. In addition, ε_r, $\tan\delta$, σ_c, and μ_c indicate the dielectric constant of the substrate, the loss tangent of the substrate, the conductivity of the conductor, and the permeability of the conductor, respectively.

The closed-form formula for the dispersive effective dielectric constant at frequency f (in Hz) is expressed as [21]

$$\varepsilon_{\mathit{eff},f} = \varepsilon_r - \frac{\varepsilon_r - \varepsilon_{\mathit{eff},0}}{1 + (f/f_x)^m} \tag{A1}$$

where

$$f_x = \frac{f_y}{0.75 + \left(0.75 - 0.332\varepsilon_r^{-1.73}\right) W/H}, \tag{A2}$$

$$f_y = \frac{4.7746 \times 10^{10}}{H\sqrt{\varepsilon_r - \varepsilon_{\mathit{eff},0}}} \tan^{-1}\left(\varepsilon_r \sqrt{\frac{\varepsilon_{\mathit{eff},0} - 1}{\varepsilon_r - \varepsilon_{\mathit{eff},0}}}\right), \tag{A3}$$

$$m = m_0 m_c, \tag{A4}$$

$$m_0 = 1 + \left(1 + \sqrt{W/H}\right)^{-1} + 0.32\left(1 + \sqrt{W/H}\right)^{-3}, \tag{A5}$$

$$m_c = \begin{cases} 1 + \frac{1.4}{1+W/H}\left[0.15 - 0.235\exp\left(\frac{-0.45f}{f_x}\right)\right] & \text{for } \frac{W}{H} \le 0.7 \\ 1 & \text{for } \frac{W}{H} > 0.7 \end{cases}. \tag{A6}$$

In [22], an accuracy better than 0.6% is claimed for all frequencies over the validity ranges: $1 \leq \varepsilon_r \leq 128$, $0.1 \leq W/H \leq 10$, and any value of H. These ranges are sufficient for practical uses. The validity of the formula has also been confirmed by experiment [23]. After the effective dielectric constant is obtained, the dispersive characteristic impedance at frequency f can be written as [24]

$$Z_{0,f} = Z_{0,0} \frac{\varepsilon_{eff,f} - 1}{\varepsilon_{eff,0} - 1} \sqrt{\frac{\varepsilon_{eff,0}}{\varepsilon_{eff,f}}} \quad (\Omega). \tag{A7}$$

In (A1) and (A7), $\varepsilon_{eff,0}$ and $Z_{0,0}$ are the static effective dielectric constant and the static characteristic impedance, respectively. Their accurate closed-form formulas are well developed and reported in [25, 26].

Attenuation in a microstrip line is caused by its dielectric loss and conductor loss, and these losses can be described by the dielectric attenuation coefficient and the conductor attenuation coefficient, respectively. The dielectric attenuation constant is frequency-dependent and its closed-form formula can be found in [26, 27] as

$$\alpha_d = 1.0472 \times 10^{-8} f \frac{\varepsilon_r}{\varepsilon_r - 1} \frac{\varepsilon_{eff,f} - 1}{\sqrt{\varepsilon_{eff,f}}} \tan\delta \quad (\text{Np/m}). \tag{A8}$$

Note that $\varepsilon_{eff,0}$ in the same equation as (A8) in [26, 27] has been replaced by $\varepsilon_{eff,f}$ here for considering the dependence on frequency. The closed-form formula for the conductor attenuation coefficient can be derived by the conformal mapping technique and appears to agree well with experimental results [26]. This formula can be written as

$$\alpha_c = \begin{cases} \dfrac{R_{DC}}{2Z_0} & \text{for } f = 0 \\ \dfrac{R_{AC,strip} + R_{AC,ground}}{2Z_{0,f}} & \text{for } f > 0 \end{cases} \quad (\text{Np/m}). \tag{A9}$$

In (A9),

$$R_{DC} = \frac{10^6}{\sigma_c W T} \ (\Omega), \tag{A10}$$

$$R_{AC,ground} = \frac{10^3}{H\left[W/H + 5.8 + 0.03\,(H/W)\right]} \sqrt{\frac{\pi f \mu_c}{\sigma_c}} \ (\Omega), \tag{A11}$$

$$R_{AC,strip} = \frac{10^3 Lr}{W} \left[\frac{1}{\pi} + \frac{1}{\pi^2} \ln\left(\frac{4\pi W}{T}\right)\right] \sqrt{\frac{\pi f \mu_c}{\sigma_c}} \ (\Omega) \tag{A12}$$

where

$$Lr = \begin{cases} 1 & \text{for } \frac{W}{H} \leq 0.5 \\ 0.94 + 0.132\frac{W}{H} - 0.0062\left(\frac{W}{H}\right)^2 & \text{for } \frac{W}{H} > 0.5 \end{cases} . \quad \text{(A13)}$$

Note that $Z_{0,0}$ in the same equation as (A9) in [26] has been replaced by $Z_{0,f}$ here. In addition, the dc resistance R_{DC} should be considered at $f = 0$. Consequently, the propagation constant obtained from (A1), (A8), and (A9) can be written as

$$\gamma = \alpha_c + \alpha_d + j2.0944 \times 10^{-8} f \sqrt{\varepsilon_{eff,f}} . \quad \text{(A14)}$$

For a dispersive and lossy microstrip line, the reflection and transmission properties can be solved by the transmission-line equations and expressed in terms of the following S-parameters:

$$S_{11} = S_{22} = \frac{Z_{0,f}^2 - Z_r^2}{Z_{0,f}^2 + Z_r^2 + 2Z_{0,f}Z_r \coth(\gamma\ell)}, \quad \text{(A15)}$$

$$S_{21} = S_{12} = \frac{2Z_{0,f}Z_r \operatorname{csch}(\gamma\ell)}{Z_{0,f}^2 + Z_r^2 + 2Z_{0,f}Z_r \coth(\gamma\ell)} \quad \text{(A16)}$$

where ℓ is the length, and Z_r is the reference impedance at ports.

REFERENCES

1. Hall, S. H., G. W. Hall, and J. A. McCall, *High-speed Digital System Design — A Handbook of Interconnect Theory and Design Practices*, Wiley, New York, 2000.
2. Young, B., *Digital Signal Integrity — Modeling and Simulation with Interconnects and Packages*, Prentice Hall, London, 2001.
3. Yee, K. S., "Numerical solution of initial boundary value problems involving Maxwell's equation in isotropic media," *IEEE Trans. Antennas Propag.*, Vol. 14, No. 5, 302–307, 1966.
4. Kunz, K. S. and R. J. Luebbers, *The Finite Difference Time Domain Method for Electromagnetics*, CRC Press, Boca Raton, FL, 1993.
5. Mardare, D. and J. LoVetri, "The finite-difference time-domain solution of lossy MTL networks with nonlinear junctions," *IEEE Trans. Electromagn. Compat.*, Vol. 37, No. 5, 252–259, 1995.
6. Taflove, A., *Computational Electrodynamics: The Finite Difference Time Domain Method*, Artech House, Norwood, MA, 1995.

7. Orlandi, A. and C. R. Paul, "FDTD analysis of lossy, multiconductor transmission lines terminated in arbitrary loads," *IEEE Trans. Electromagn. Compat.*, Vol. 38, No. 3, 388–399, 1996.
8. Djordjevic, A. R., T. K. Sarkar, and R. F. Harrington, "Analysis of lossy transmission lines with arbitrary nonlinear terminal networks," *IEEE Trans. Microwave Theory Tech.*, Vol. 34, No. 6, 660–666, 1986.
9. Schutt-Aine, J. E. and R. Mittra, "Scattering parameter transient analysis of transmission lines loaded with nonlinear terminations," *IEEE Trans. Microwave Theory Tech.*, Vol. 36, No. 3, 529–539, 1988.
10. Winklestein, D., M. B. Steer, and R. Pomerieau, "Simulation of arbitrary transmission line networks with nonlinear terminations," *IEEE Trans. Circuit Syst.*, Vol. 38, No. 4, 418–422, 1991.
11. Komuro, T., "Time-domain analysis of lossy transmission lines with arbitrary terminal networks," *IEEE Trans. Circuit Syst.*, Vol. 38, No. 10, 1160–1164, 1991.
12. Chang, F. Y., "Waveform relaxation analysis of nonuniform lossy transmission lines characterized with frequency-dependent parameters," *IEEE Trans. Circuit Syst.*, Vol. 38, No. 10, 1484–1500, 1991.
13. Gu, Q., D. M. Sheen, and S. M. Ali, "Analysis of transients in frequency-dependent interconnections and planar circuits with nonlinear loads," *IEEE Proc.-H*, Vol. 139, No. 2, 38–44, 1992.
14. Mao, J. F. and Z. F. Li, "Analysis of the time response of nonuniform multiconductor transmission lines with a method of equivalent cascaded network chain," *IEEE Trans. Microwave Theory Tech.*, Vol. 40, No. 5, 948–954, 1992.
15. Maio, I., S. Pignari, and F. Canavero, "Influence of the line characterization on transient analysis of nonlinearly loaded lossy transmission lines," *IEEE Trans. Circuit Syst. I*, Vol. 41, No. 3, 197–209, 1994.
16. Huang, C. C., "Analysis of multiconductor transmission lines with nonlinear terminations in frequency domain," *Journal of Electromagnetic Waves and Applications*, Vol. 19, No. 8, 1069–1083, 2005.
17. Antonini, G., "A dyadic Green's function based method for the transient analysis of lossy and dispersive multiconductor transmission lines," *IEEE Trans. Microwave Theory Tech.*, Vol. 56, No. 4, 880–895, 2008.
18. Chiang, I. T. and W. C. Chew, "Fast real-time convolution

algorithm for microwave multiport networks with nonlinear terminations," *IEEE Trans. Circuit Syst. II*, Vol. 52, No. 7, 370–375, 2005.

19. Chiang, I. T. and W. C. Chew, "Fast real-time convolution algorithm for transients of nonlinearly-terminated microwave multiport circuits," *Microwave Opt. Tech. Lett.*, Vol. 39, No. 4, 280–282, 2003.
20. Hairer, E., C. Lubich, and M. Schliche, "Fast numerical solution of nonlinear Volterra convolution equations," *SIAM J. Sci. Stat. Comput.*, Vol. 6, 532–541, 1985.
21. Edwards, T. C. and M. B. Steer, *Foundations of Interconnect and Microstrip Design*, Wiley, New York, 2000.
22. Kobayashi, M., "A dispersion formula satisfying recent requirements in microstrip CAD," *IEEE Trans. Microwave Theory Tech.*, Vol. 36, No. 8, 1246–1250, 1988.
23. York, R. A. and R. C. Compton, "Experimental evaluation of existing CAD models for microstrip dispersion," *IEEE Trans. Microwave Theory Tech.*, Vol. 38, No. 3, 327–328, 1990.
24. Hammerstad, E. and O. Jensen, "Accurate models for microstrip computer-aided design," *IEEE MTT-S Int. Microwave Symp. Dig.*, 407–409, 1980.
25. Bahl, I. J. and R. Garg, "Simple and accurate formulas for a microstrip with finite strip thickness," *Proc. IEEE*, Vol. 65, No. 11, 1611–1612, 1977.
26. Collin, R. E., *Foundations for Microwave Engineering*, 2nd edition, McGraw-Hill, New York, 1992.
27. Denlinger, E. J., "Losses of microstrip lines," *IEEE Trans. Microwave Theory Tech.*, Vol. 28, No. 6, 513–522, 1980.